GROUND RUN MANEUVERING QUALITIES OF AIRCRAFT WITH NOSE WHEEL CONTROL

S. Luthander[+] L. Wickström[++] S. Öberg[+++]

LUTAB. Consultants, Scientific and Technical Projects, Bromma, Sweden

ABSTRACT

Based on the existing framework of vehicle dynamics theory a structure is suggested for the ground run maneuvering qualities problem combining two related areas referred to as response and phase optimization. A survey simulation program covering mainly the response problem area has been conducted in the FOSIM research simulator adapted to ground run tests at a constant speed of 50 m/s. Emphasis has been on fighter type aircraft of the 10-15 ton class with the aim to define vehicle parameter values corresponding to satisfactory respectively unacceptable pilot rating of the ground run maneuvering qualities.

1. INTRODUCTION

In order to keep an aircraft on the comparatively narrow runway the pilot must compensate for disturbances by control actions. Examples are: Initial errors at touch down, strong side gusts, asymmetric forces due to thrust reverser and brake action. Thus a maneuverability problem exists for the ground run in spite of the straight path.

In absence of specifications and design recommendations referring to this problem it has been considered worth while to make a brief study of the problem. The paper gives a short account of results from a survey mapping of various parameter effects on the ground run maneuvering qualities by means of simulation runs in the FOSIM research flight simulator (ref. 4,5)

2. MANEUVERING QUALITIES (MQ) STRUCTURE

2.1 Two degrees of freedom equations

The maneuvering qualities structure can be described with reference to the two-dimensional equations for vehicle dynamics (ref 1-3). (Table 2-4.)

The characteristic equation of this system defines eigenvalues (ω_0, ζ). Depending on the numerical relationships between the coefficients of this equation the eigenmotion is of one of the following types

- periodic, damped ($\omega^2_0 > 0$, $0 < \zeta < 1$)
- aperiodic damped (2 subsidences; $\omega^2_0 > 0$, $1 < \zeta < \infty$)
- aperiodic divergent (1 subsid, 1 diverg; $\omega^2_0 < 0$)

A vehicle that is divergent in the side-yaw eigenmotion (i.e. has ground loop tendency) is not wanted. Therefore $\omega^2_0 < 0$ must be exluded.

2.2 The MQ structure

2.21 General

It follows that the main structure of the maneuvering quality problem can be described in four steps by reference to Fig 1:

(1) First, if system eigenvalues (ω_0, ζ) are stipulated a point is defined in the coordinate system

(2) Then we consider the two additional parameters (K_r, T_r) in the r - equation which is the primary equation for yaw control. Here (Table 2)

- $K_r = \dot{r}(0)/\delta$ is the control gain, it also is the initial control yaw acceleration response to step input; and
- $1/T_r\omega_0$ is the ratio between the inverse lead time constant, and the system eigenfrequency.

(3) Next we consider the parameters related to the β-equation, these can be defined as

- $\alpha = K_\beta/K_r$ which relates the β-equation to the r-equation; and
- $D = \alpha/T_\beta$ which representents the specific character of the vehicle dynamics which is due to the β-equation.

(4) Finally consequenses of additional degrees of freedom i. e. roll angle and landing gear cinematics will have to be considered in some cases for checks or modifications of conclusions based on two-dimensional analysis.

2.22 The parameter α

The parameter α has the significance of an initial control response ratio (Table 2)

$$\alpha = K_\beta/K_r = \left[\dot{\beta}(0)/\delta\right] / \left[\dot{r}(0)/\delta\right] \qquad [\text{sec}]$$

Expressing K_β and K_r in design parameters gives the general formula

$$\alpha = (I_z/mU) \cdot Y_\delta/N_\delta \qquad \text{(general definition)}$$

For nose-wheel control the following relation holds, if aerodynamic forces are neglected

$$N_\delta = Y_\delta \cdot a$$

Thus, for nose-wheel control

$$\alpha = I_z/mUa \qquad \text{(ground friction forces only)}$$

Typical orders of magnitude for a 10 tons aircraft with nose-wheel control are

$m = 10^4$ kg, $I_z = 10^5$ kg m^2, $a = 5$ m, $U = 50$ m/s which gives $\alpha = 0.04$ i.e. $\alpha \ll 1$.

(This does not apply for all-wheel control where α can be made zero)

2.23 Response optimization

If α and D are stipulated in addition to ω_0 and ζ, the vehicles maneuvering qualities can be assessed for each combination of K_r and $1/T_r\omega_0$. Then the following problem is defined

---

[+]Professor of Aeronautics, Ret, The Royal Inst of Technology, Stockholm. [++]Research engineer, FOSIM Research Flight Simulator. [+++]Research engineer, Vehicle Dynamics.

•find optimum combinations of K_r and $1/T_r\omega_0$, i.e combinations giving satisfactory pilot rating of the maneuvering quality (MQ); and

•find danger areas, i.e. combinations for which MQ is rated unacceptable by pilots.

This problem is illustrated in Fig 2.

The reason why the designation 'response optimization' is used is the evident significance of the pertinent variables (Table 2)

$K_r = \dot{r}(0)/\delta$ = initial control response

$K_r/T_r\omega_0^2 = r(\infty)/\delta$ = steady state control resp.

In the small top diagram in Fig 2 radial lines are included, indicating values of

$r(\infty)/\dot{r}(0)$ = control response ratio.

Optimum control harmony occurs for certain combinations of these response parameters. Included in the diagram are also typical curves for PR = Const. Along such a curve all of the three response characteristica mentioned varies, still in such a way that the pilot is willing to compromize the same over all rating of the maneuvering quality.

(The pilots rating situation when optimizing K_r or evaluating PR is illustrated in Fig A-1 (Appendix). Obviously the pilots emphasis has to be on different dynamic parameters in different sectors of the response diagram).

The pilots adaption to the closed loop $\psi - \delta$ - system occurs with minimum pilot compensation (corresponding to optimum pilot rating of MQ) when $T_r\omega_0$ is adjusted to ζ in a certain way that implies good servotechnical quality of the closed control loop. The controlled system optimum adaption is independent of ω_0. The pilot, however, is independent of ω_0 only within limits.

Therefore a diagram of the type shown on Fig 2 (top) may be expected to be valid only within a range of ω_0 -values around some human-pilot-related optimum of ω_0, and to show declining PR -values above and below this range. Such a diagram is illustrated schematically in more detail in Fig 3 and will now be further discussed.

Niveau-lines for PR = const in the plane ζ = const are shown in Fig 3a with the coordinates

$(K_r, 1/T_r\omega_0)$, and in Fig 3b with the coordinates

$(K_r, K_r/T_r\omega^2)$(or $\dot{r}(0)/\delta$; $r(\infty)/\delta$).

In Fig 3c is shown one way of defining an optimum value of K_r (line aa), namely the value of K_r that for a given value of PR makes $1/T_r\omega_0$ maximum and minimum. The significance of this will be discussed below.

In Fig 3d is shown a three-dimensional surface PR = constant, the maneuvering qualities space and its crossection with a plane ζ = constant. The projections on the coordinate planes (K_r = 0 and $1/T_r\omega_0$ = 0) of the surface PR = const (=6) are also indicated. This means, that the line aa is projected on the plane K_r = 0, but that the line bb is projected on the plane $1/T_r\omega_0$ = 0 (Compare Fig 3c, where the line aa is projected also on the plane $1/T_r\omega_0$ = 0).

We now consider Fig 4, where lines aa, bb, and cc are indicated. These lines have following meaning

aa defines	max and min of	$r(\infty)/\dot{r}(0)$	at PR = const
bb	-"-	$\dot{r}(0)/\delta$	-"-
cc	-"-	$r(\infty)/\delta$	-"-

From this discussion follows

- If lines for PR = const are presented as in Fig 3d in either of the planes K_r = 0 and $1/T_r\omega_0$ = 0 there are in each case at least three different ways to define the lines, namely corresponding to values of K_r which give alternatively

optimum in $r(\infty)/\dot{r}(0)$ (proj. of line aa); or

-"- $\dot{r}(0)/\delta$ (proj. of line bb); or

-"- $r(\infty)/\delta$ (proj. of line cc).

A presentation of the maneuvering qualities in a two-dimensional MQ-plane therefore is not unambiguous without specification of which of these (or other) cases that is understood.

One way of getting around or solving this complication and define in an unambiguous way a maneuvering qualities plane is illustrated in Fig 5 and will now be discussed.

In this case the first task of the simulator pilot is to optimize the value of K_r, the other configuration parameters given (and not to assign the PR-ratings, this beeing done later in special simulator runs).

This two-stage evaluation is illustrated in Fig 5. In Fig 5a is shown the first - evaluated pilot-optimized value of K_r, written as K_r^*. In Fig 5b is shown the result of a PR-evaluation, for each configuration performed with only one value of K_r, namely equal to the corresponding value of K_r^*.

The two groups of niveau-lines for K_r^* = const and for $PR(K_r^*)$ = const in Fig 5a,b can be superimposed in one $(1/T_r\omega_0, \zeta)$ -plane, thus forming a compact presentation of the maneuvering qualities for the set of pilot-optimized configurations.

2.24 Phase optimization

If the yaw motion equation parameters (i.e. ω_0, ζ, K_r, T_r) are assumed stipulated for a vehicle having a stipulated value of the parameter α, the vehicle maneuvering qualities are depending on the parameter T_β in the side motion equation. There are several different composite parameters which include T_β and which are useful from different viewpoints in correlating the pilot ratings of maneuvering qualities, as far as T_β -effects are concerned. Some of these related parameters are

(1) $D = \alpha/T_\beta$

(2) $K_\zeta = (1+D)/(\alpha \cdot 2\zeta\omega_0)$

(3) $\beta(\infty)/r(\infty) = T_r\omega_0 \cdot D \cdot 1/\omega_0$

(4) $\angle\tilde{\beta}/\tilde{\delta}$ phase lag at stipulated $\omega_1 < \omega_0$

Consequently, also in this case the following problems are defined

•find the values of the T_β -related parameter that gives satisfactory pilot rating (PR) of the maneuvering qualities (MQ); and

•find danger areas, i.e. values of the T_β -related parameter for which MQ is rated unacceptable by the pilots.

This problem is illustrated in Fig 6. The designation 'phase optimization' has been used here as the adverse affects of the T_β -influence is strongly related to the phase lag of the β-motion behind the ψ-motion,

In the top diagram in Fig 6 curves for constant values of parameter (4) (i.e. $\angle\tilde{\beta}/\tilde{\delta}$ at $\omega_1 = \omega_0/2$) are indicated as an example of one of several corre-

lation parameters possible for pilot ratings of the maneuvering qualities.

2.25 Simulation structure

The maneuvering qualities structure discussed in previous sections is background for a simulation structure shown in Fig 7. Here Part 1 corresponds to response mapping with the steps

1. Stipulate ζ, ω_0
2. Stipulate D or K_ζ or $\beta(\infty)/r(\infty)$
3. Find PR(K_r; $1/T_r\omega_0$; D) by simulation tests
4. Repeat with other D, ζ, ω_0;

and Part 2 corresponds to phase mapping with the steps

1. Stipulate ζ, ω_0
2. Stipulate K_r
3. Find PR(D; $1/T_r\omega_0$; K_r) by simulation tests
4. Repeat with other K_r, ζ, ω_0.

Typical results from Part 1 - simulations will be described below. Simulation results from Part 2 are not available to the same extent, however, some limited results are also presented below.

3. SURVEY OF SIMULATION RESULTS, AND PRELIMINARY DESIGN SUGGESTIONS+

3.1 The reference configuration

($\omega_0 = 1.5$, $K_\zeta = 0.4$, $\alpha = 0.05$, $U = 50$ m/s)

3.11 The control gain

Pilot-optimized values of $K_r^*(S_1 S_2 S_3)$ obtained by simulation tests are shown in Fig 8 for the damping range $0.2 < \zeta < 1.8$.

Assuming that at given combination of ζ and $T_r\omega_0$ there is a value of K_r that could provide good maneuvering qualities, then this optimum K_r should correspond to an optimum phase margin (Φ_{PM}) in the open loop pilot-vehicle system, and in a simulation set up the pilot would probably ask for such a value of K_r. In this situation the pilot would be 'non-compensating' and a good approximation for his transfer function may be

$$\tilde{Y}_p = K_p \cdot e^{-\tau s} \qquad (\tau \doteq 0{,}3)$$

Therefore, in order to illustrate how K_r depends on ζ and $1/T_r\omega_0$ the value of K_r has been computed that corresponds to a prescribed value of the phase margin (Φ_{PM}) for the open-loop pilot-vehicle system

$$\tilde{Y} = \tilde{Y}_p \cdot \tilde{X}/\tilde{\delta}$$

Fig 9 shows the value of K_r that corresponds to zero phase margin. As this is the stability limit it is the theoretical maximum of K_r. Still, for a real vehicle larger values can be desirable if large disturbances occur.

Comparison of Fig 8 and Fig 9 shows a general agreement concerning the structure of the functions K_r^* and $K_r(\Phi_{PM} = 0)$. We conclude that the typical relation between $K_r, \zeta, T_r\omega_0)$ at optimum K_r can be obtained from curves for constant phase margin.

The experimental curves for $K_r^* = \text{const}$ in the plane $K_r^* = 0$ in Fig 8 indicate that for large values of ζ the pilot has two control modes, one at small $1/T_r\omega_0$ (decreasing K_r^* for increasing $1/T_r\omega_0$), and another at large $1/T_r\omega_0$ (increasing K_r^* for increasing $1/T_r\omega_0$).

+ The simulations were performed with following Control System Characteristics (Appendix)
$\partial F_s/\partial X_s = 50$ N/cm $\quad \partial F_s/\partial\delta = 350$ N/rad

In Table 2 is indicated that the parameter K_r also defines the initial and the steady state yaw control responses according to the formulas

$$\dot{r}(0)/\delta = K_r \qquad r(\infty)/\delta = K_r/T_r\omega_0^2$$

From these definitions it follows that the lines for $K_r = \text{const}$ in the plane (ζ ; $1/T_r\omega_0$) in Fig 8,9 also indicate the initial response ($\dot{r}(0)/\delta$) and that lines for the steady state response can be computed from K_r and $1/T_r\omega_0$ (ω_0 is stipulated).

Such control response diagrams are presented in Fig 10a,b which correspond to Fig 8,9. The abscissa can be written either as $1/T_r\omega_0$ or as

$$r(\infty)/\dot{r}(0) = 1/T_r\omega_0 \cdot 1/\omega_0$$

which indicates the control response ratio.

3.12 The pilot ratings (PR)

The value of pilot rating of maneuvering qualities corresponding to K_r^* (and evaluated by the same pilot which evaluated K_r^* in Fig 8) is shown in Fig 11. This figure is based on ratings at small control maneuvers (PR_{sm}) and a similar figure (not shown) is obtained for large control maneuvers (PR_{st}).

A composite diagram, of type of Fig 5, of K_r from Fig 8 and PR_{sm}, PR_{st} from Fig 11 is shown in Fig 12a,b.

This defines the maneuvering qualities plane for the reference configuration. It may be remarked that the figure is conditioned by two special facts

- K_r^* and PR have been evaluated under the specific disturbances $S_1 S_2 S_3$; and
- the diagrams are based on tests with one pilot only and on only 10 test runs.

3.2 Complementary study of the reference configuration at $\zeta = 0{,}6$ and the FT-distinction

Using the FT-distinction (Appendix Sect 2.2) for pilot rating the niveau-charts in Fig 13 and 14 (which is obtained from Fig 13 by multiplying the abscissa by K_r/ω_0) have been obtained by a series of simulations for the function

PR (K_r; $1/T_r\omega_0$; S_3) (The PR = 6 curve is shown by curves A in Fig 15)

Similar charts (not shown) where also evaluated by another series of simulations for the function

PR ($1/T_r\omega_0$; K_r; S_3) (The PR = 6 curve is shown by curves B in Fig 15)

One should have expected these two sets of niveau-charts to be equal. However, due to limited accurace and repeatability of the evaluation and also because of the comparatively low number of tests some differences were obtained in spite of the fact that the same pilot made the test runs and the ratings behind both the niveau-charts. (The total number of test runs/test points was: for Fig 15A: 41, with 4 values of $1/T_r\omega_0$ and for Fig 15B: 41, with 5 values of K_r.)

The result, however, is seen to define a function of the type indicated in Fig 3 for a plane $\zeta = \text{const}$ in the maneuvering qualities space.

3.3 Results of parameter variations

($K_\zeta = 0.4$, $\alpha = 0{,}05$, $U = 50$m/s)

(without referring to the simulations performed)

3.31 Eigenfrequency and damping

Suggested requirements (prelim) on ω_0 at $\zeta \doteq 0.6$:

Maneuvering Quality	ω_0
Satisfactory	$3 < \omega_0$
Acceptable	$1.25 < \omega_0 < 3$
Unacceptable	$\omega_0 < 1.25$

Suggested requirements (prelim) on ζ at $\omega_0 \doteq 1.5$

Maneuvering Quality	Disturbances	
	Large	Moderate
Satisfactory	$1.5 < \zeta$	$0.5 < \zeta$
Acceptable	$0.4 < \zeta < 1.5$	
Unacceptable	$\zeta < 0.4$	

A suggested (prelim) composite diagram for requirements on ω_0 and ζ is shown in Fig 16.

3.32 Control authority and control response ratio

Pilot-preferred values (prelim) of the control authority ($\omega_0 = 1.5$ $\zeta = 0.6$ $K_\zeta = 0.4$ $\alpha = 0.05$ $U = 50$ m/s) read from Fig 15 are

Type of aircraft	$K_r = \dot{r}(0)/\delta$ at 50 m/s [1/sec]		
	min (PR=6)	opt	max (PR=6)
Fighter	0.5	1.9	(3.5)
Transport	0.4	0.6	2.5

Pilot-preferred values (prelim) of the control response ratio (parameters as above) read from Fig 15 are

Type of aircraft	$R = r(\infty)/\dot{r}(0) = 1/T_r\omega_0$ [sec]		
	min (PR=6)	opt	max (PR=6)
Fighter	0.25	0.5	0.75
Transport	0.2	0.5	0.8

3.33 Understeer ratio

For a neutral steer vehicle the steady state yaw rate response is defined by

$$r(\infty)/\delta = U/l = K_{r_0}/T_r\omega^2_0$$

The pilot-preferred value of K_r^* compared to this neutral steer reference value K_{r_0} is found to increase with ζ and $1/T_r\omega_0$. At $\zeta \doteq 0.6$ $U = 50$ m/s is obtained

$$0.06 < K_r^*/K_{r_0} < 0.11 \qquad (0.5 < 1/T_r\omega_0 < 3)$$

3.4 Discussion of the K_ζ -effects

3.41 Definitions (Table 2)

The parameter K_ζ is related to effects from the side slip equation and is associated with (the first order term in the nominators of) the transfer function to heading angle (and to side acceleration) from the nose wheel angle (related parameters are D and $\beta(\infty)/r(\infty)$, see 2.24)

It is remarked here that in real world vehicle driving both visual cues from heading angle and kinestetic cues from side acceleration forces are imposed upon the pilot, while in the present simulations the latter cues were deleted as the simulator motion system did not include the side motion.

3.42 Survey of K_ζ -effects

A survey of K_ζ -effects on K_r^* and $PR(K_r^*)$ as functions of $1/T_r\omega_0$ and ζ is shown in Fig 17 and 18 for the configuration $\omega_0 = 1.5$ $\alpha = 0{,}05$. For the sake of clearness niveau curves are included in Fig 18 only for PR = 3 and 6 (test points omitted).

K_r^* is seen to increase with increasing ζ and with decreasing K_ζ. This will be discussed below.

3.43 Transient responses

A pronounced effect of K_ζ is demonstrated in the transient responses to step control input (Fig 19). Thus, a low value of K_ζ gives a very sluggish transient response.

3.44 The control gain

The simulation series presented in Fig 17, 18 also show noticeable effects of K_ζ.

The pilot-optimized control gain (K_r^*) was found to be increased for reduced values of K_ζ. This is shown in Fig 20 which extracts information from Fig 17.

The trend can be understood as a consequence of the sluggish transient response. In order to attain a desired transient response, say 1 sec after application of a step control input (compare Fig 19e), the pilot has to compensate for the sluggishness of a low-K_ζ-system by using an increased control gain.

3.45 The pilot ratings

The pilot ratings (PR) of the maneuvering quality also was evaluated in the simulation series mentioned above, using the pilot-optimized gain. The result is illustrated in Fig 18.

These diagrams indicate that the minimum of the curves PR = const is moved towards higher $1/T_r\omega_0$ when K_ζ is decreased. This is shown more clearly in Fig 21 that presents values of $1/T_r\omega_0$ for optimum PR at constant values of ζ.

This effect is, hypothetically, related to the β-equation influence which is evident in two forms

- as a skidding tendency during maneuvering; and
- as an increase of the phase lag between the control input and the heading angle output.

These effects are discussed below.

3.46 Skidding effects

From Fig 19 is seen that two K_ζ-related β-effects are rather pronounced, namely

- the negative maximum of $\dot{\beta}/\delta$ during the early stage of the transient response to step control input; and
- the steady state side angle response to step control input ($\beta(\infty)/\delta$).

The side angle, which is the difference between the heading angle and the yaw angle, is perceived by the pilot as a skidding, which may be very disturbing if too large, and which therefore affects the pilot's ratings of the maneuvering quality.

From Fig 19 is concluded that $(\dot{\beta}/\delta)_{min}$ which occurs early in the transition phase, probably is the most suitable correlation parameter for PR_β (the pilots perception of difficulty due to β). Since, however, the analytical expression for $\dot{\beta}/\delta$ is complicated, the other β-effect ($\beta(\infty)/\delta$) has been used here to define a correlation parameter for the pilot rating.

For this purpose the ratio between the steady state control responses in side angle and yaw rate is introduced as a skidding parameter

$$\beta(\infty)/r(\infty) = K_\beta T_r/K_r T_\beta$$

Introducing the definition of K_ζ and solving for T_β this can be written as

$$\beta(\infty)/r(\infty) = -T_r(1-2\zeta\omega_0 K_\zeta K_\beta/K_r)$$

This relationship is illustrated in Fig 22 which shows that the skidding parameter is increased for decreasing value of $1/T_r\omega_0$ and for decreasing value of ω_0. A secondary influence have ζ and K_ζ and decreasing these parameters increases the skidding parameter.

Results of simulation tests on pilot rating (PR_β) of the skidding parameter are shown in Fig 23.

It may be concluded, somewhat arbitrarily, that requirements on the skidding parameter could be suggested as below

Suggested requirements on $\beta(\infty)/r(\infty)$ (preliminary)

Maneuvering Quality	Skidding parameter
Satisfactory	$\beta(\infty)/r(\infty)<1$
Acceptable	$1<\beta(\infty)/r(\infty)<4$
Unacceptable	$4<\beta(\infty)/r(\infty)$

These suggested requirements are translated into approximative ranges of $1/T_r\omega_0$ in Fig 24. In doing this Fig 22 has been used and the factor $(1-\Delta) = 1$ conservatively assumed.

The above mentioned formula for the skidding parameter, illustrated in Fig 22 can also be presented as in Fig 25 with the coordinates $1/T_r\omega_0$ and K_ζ. This figure should be compared to Fig 21 which is designed in these coordinates. As large values of the skidding parameter is a degrading factor when rating the maneuvering quality (see above) it seems plausible that locus for PR_{opt} in Fig 21 is nearly related to locus for a low value of the skidding parameter. As seen from Fig 25 this also is the case.

3.47 The phase lag effects

The phase lag of heading angle to visual input signal for the pilot-vehicle combination is illustrated in Fig 26. This figure illustrates the influence of the parameters K_ζ, ζ and $1/T_r\omega_0$. The phase lag is increased by

- decreasing of K_ζ; and by
- increasing of ζ.

The phase lag of side angle to control input for the vehicle alone has been computed for $\omega_1 = \omega_0/2$ and presented as a function of the parameter $1/T_r\omega_0$. The effect of K_ζ on this relationship is illustrated in Fig 27 for the configuration $\omega_0 = 1.5$ $\zeta = 1.0$ $\alpha = 0.05$.

The figure shows that if $K_\zeta > 5$ the phase lag is below 10^o and can be expected to be hardly perceptible to the pilot. In this case the phase lag also is nearly constant over the $1/T_r\omega_0$-range.

On the other hand, if K_ζ is small (i.e. $K \doteq 0.4$) the phase lag has a maximum of 60^o at low values of $1/T_r\omega_0$. In this case the phase lag is reduced as $1/T_r\omega_0$ is increased and becomes of the order 20^o (i.e. probably acceptable to the pilot) at $1/T_r\omega_0 > 1.5$

The data in Fig 27 have been presented in another way in Fig 28. Assuming hypothetically that a phase lag of 20^o is acceptable to the pilot, this figure would again support the type of data presented in Fig 21.

It may be noted that Fig 28 is the type of presentation of the parameter α/T_β that was chosen in the presentation of the 'phase-optimization' problem in Fig 6.

Unfortunately the time allowed for the simulation runs did not permit mapping of PR = const-lines in a diagram of type as in Fig 28.

4. SUMMARY

A structure of the maneuvering quality problem has been suggested in section 2 above and in section 3 numerical results from simulation tests have been surveyed as illustrations.

In two degrees of freedom the maneuvering quality is dependent on six vehicle dynamic parameters ($\omega_0, \zeta, K_r, T_r, K_\beta, T_\beta$, see Table 4)

The simulation study, which has been conducted at one speed only (50 m/s), has resulted in suggested recommendations (preliminary) for the numerical values of these parameters. The numerical values refer to two levels of pilot acceptance: satisfactory respectively acceptable. For the parameter T_β lack of systematic simulation test data makes the results and conclusions less distinct than for the other parameters.

In an Appendix comments are made on the simulation technique and on the consistency of evaluations. Important factor is the disturbance spectrum.

In a Supplement degrading factors for the ground run maneuvering qualities are listed and briefly discussed. Important factor is the vertical wheel load redistribution due to wheel braking and to thrust reverser effects.

ACKNOWLEDGEMENT

This paper is abridged from ref 5, which was performed under contract with the Air Material Department in the Swedish Defence Material Administration and the permission for publication is acknowledged.

Acknowledgements are also due to Mr. Bo d'Ailly, AMA, Mr. Milton Mobärg, SAAB, and Captain Petrus Ericsson, SAS, for useful comments and discussions and to the participating simulation pilots.

REFERENCES

1. Design implications of a general theory of automobile stability and control, by D.W. Whitcomb and W.F. Milliken jr. Proc. Autom. Div. Inst. Mech. Eng. 1956-57 p. 367-425.

2. Vehicle Dynamics, by J.R. Ellis, London Business Books Ltd, 1969.

3. Dynamics of the automobile related to driver control, by D.H. Weir, C.P. Shortwell, W.A. Johnson. Systems Technology Inc., Technical Report No 157-1.

4. The Flight Research Simulator FOSIM. KTH Aero Memo FI 182 (1975). Dept of Aeron., The Royal Inst. of Technology, Stockholm.

5. Maneuvering qualities during aircraft ground run. Results and conclusions from a simulator study. LUTAB Report TA 732-R3 (1975).

6. Appendix I to Calspan report BM-3054-F1, p. 287--291.

Table 1. Nomenclature

Vehicle

- m mass
- l length front wheel to rear wheel
- a distance front wheel to center of gravity (CG)
- b distance center of gravity to rear wheel
- I_z moment of inertia for CG
- α $I_z/(mUa)$
- δ nose wheel steer angle

Motion

- β side angle U-vector vs vehicle center line
- r yaw angle rate
- U ground run speed
- U_L landing speed
- a_x, a_y longitudinal, lateral acceleration

Forces

- F_z vertical wheel reaction force
- Y lateral force
- N yawing moment
- S_F, S_R side friction force on front, rear wheel perpendicular to its plane
- ϵ_F, ϵ_R angle between wheel plane and velocity vector of wheel hub
- C_F, C_R cornering power of front, rear wheel

Derivatives

$Y_\beta = \partial Y/\partial\beta$, $Y_r = \partial Y/\partial r$

$N_\beta = \partial N/\partial\beta$, $N_r = \partial N/\partial r$

Aerodynamics

- ϱ density of air
- S reference area
- c_{ref} reference length
- C_n yawing moment coefficient
- C_y lateral force coefficient

Static Stability

- NP neutral point (lateral)
- NP_μ d:o, only ground friction forces considered
- a_{NP} distance front wheel - NP
- a_{NP_μ} d:o front wheel - NP_μ
- SM static margin; $SM \cdot l = a_{NP} - a$
  $SM_\mu \cdot l = a_{NP_\mu} - a$
  $a_{NP_\mu}/l = 1/(1+C_F/C_R)$

Dynamics

- K_r, K_β gains
- T_r, T_β time constants
- ω_0 frequency } side yaw eigenvalues
- ζ rel.damping } side yaw eigenvalues

(See Tables 2-4)

Control (See Appendix)

- F_s, X_s pedal force, displacement

Simulation (See Appendix)

- $S_1 S_2 S_3$ disturbance types during simulated ground run
- PR pilot rating of ground run maneuvering qualities

Table 2 Two-dimensional equations for vehicle motion

General form

$$\begin{cases} mU\dot{\chi} = Y \ ; \ \chi = \psi + \beta \\ I_z \dot{r} = N \ ; \ r = \dot{\psi} \end{cases}$$

Stability derivative form

$$\begin{cases} \dot{\beta} - Y_\beta/mU \cdot \beta - (1 - Y_r/mU) \cdot r = Y_\delta/mU \cdot \delta + Y_D/mU \\ -N_\beta/I_z \cdot \beta + \dot{r} - N_r/I_z \cdot r = N_\delta/I_z \cdot \delta + N_D/I_z \end{cases}$$

Frequency response form

$$\begin{cases} \tilde{\beta}/\tilde{\delta} = K_\beta (s + 1/T_\beta) / (s^2 + 2\zeta\omega_0 s + \omega_0^2) \\ \tilde{r}/\tilde{\delta} = K_r (s + 1/T_r) / (s^2 + 2\zeta\omega_0 s + \omega_0^2) \end{cases}$$

It follows $(\alpha = K_\beta/K_r)$

$$\frac{\dot{r}(0)}{\delta} = K_r \quad \frac{r(\infty)}{\delta} = \frac{K_r}{T_r \omega_0^2} \quad \frac{\dot{\beta}(0)}{\dot{r}(0)} = \alpha \quad \frac{\beta(\infty)}{r(\infty)} = \alpha \frac{T_r}{T_\beta}$$

$$\frac{\dot{\beta}(0)}{\delta} = K_\beta \quad \frac{\beta(\infty)}{\delta} = \frac{K_\beta}{T_\beta \omega_0^2} \quad \frac{r(\infty)}{\dot{r}(0)} = \frac{1}{T_r \omega_0^2} \quad \frac{\beta(\infty)}{\dot{\beta}(0)} = \frac{1}{T_\beta \omega_0^2}$$

and

$$\tilde{\chi}/\tilde{\delta} = K_\beta (s^2 + K_\zeta 2\zeta\omega_0 s + K_\omega \omega_0^2) / (s^2 + 2\zeta\omega_0 s + \omega_0^2)$$

$$K_\zeta \cdot 2\zeta\omega_0 = 1/\alpha + 1/T_\beta \qquad K_\omega \cdot \alpha = 1/T_r \omega_0^2)$$

Table 3 Friction force (index μ) and aerodynamic force (index a) derivatives

$Y_{\mu\beta} = C_F + C_R$	$Y_{a\beta} = C_{y\beta} \cdot S U^2 \varrho/2$	$N_{\mu\beta} = a C_F - b C_R$	$N_{a\beta} = C_{n\beta} \cdot S c_{ref} U^2 \varrho/2$
$Y_{\mu r} = (a C_F - b C_R)/U$	$Y_{ar} = C_{yr} \cdot S c_{ref} U \varrho/2$	$N_{\mu r} = (a^2 C_F + b^2 C_R)/U$	$N_{ar} = C_{nr} \cdot S c^2_{ref} U \varrho/2$
$Y_{\mu\delta} = -C_F$	$Y_{a\delta} = C_{y\delta} \cdot S U^2 \varrho/2$	$N_{\mu\delta} = -a C_F$	$N_{a\delta} = C_{n\delta} \cdot S c_{ref} U^2 \varrho/2$

Table 4 Transfer function parameters expressed in derivatives (a+μ) and in vehicle parameters (μ)

(a+μ)	$K_r = N_\delta/I_z$	$K_\beta = Y_\delta/mU$	$1/T_r = -Y_\beta/mU + N_\beta/mU \cdot Y_\delta/N_\delta$	$1/T_\beta = -N_r/I_z - (mU - Y_r)/I_z \cdot N_\delta/Y_\delta$
	$2\zeta\omega_0 = -(Y_\beta/mU) + N_r/I_z$		$\omega_0^2 = N_\beta/I_z - Y_r/mU \cdot N_\beta/I_z + Y_\beta/mU \cdot N_r/I_z$	
(μ)	$K_r = -a C_F/I_z$	$K_\beta = -C_F/mU$	$1/T_r = -C_R/mU \cdot l/a$	$1/T_\beta = -mUa/I_z - bl C_R/U I_z$
	$2\zeta\omega_0 = -(C_F(I_z + ma^2) + C_R(I_z + mb^2)) \cdot 1/mUI_z$		$\omega_0^2 = (a C_F - b C_R) \cdot 1/I_z + C_F C_R l^2/mU^2 I_z$	

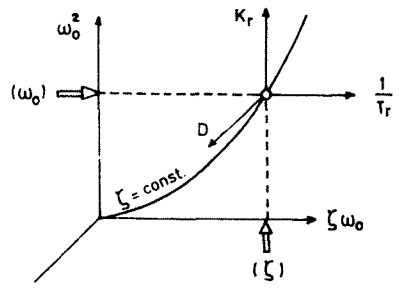

Fig 1.
Two degrees of freedom
- yaw angle
- side angle

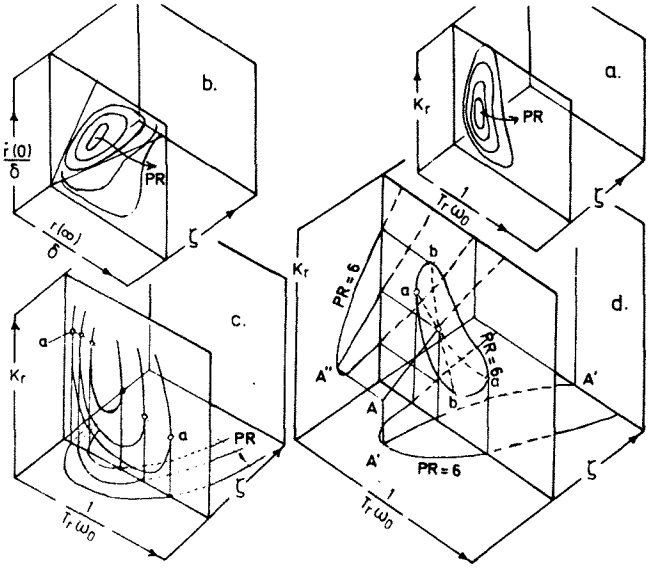

Fig 3. a. General Diagram b. Response Diagram
c. Optimum K_r (regarding $r(\infty)/\dot r(0)$) d. Rating Surfaces PR = Const.

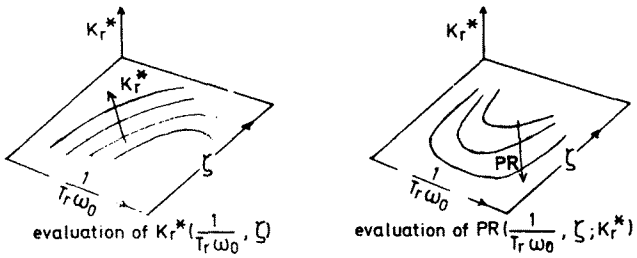

Fig 5. Maneuvering Qualities Plane for optimum system based on pilot-optimized gain (K_r^*)

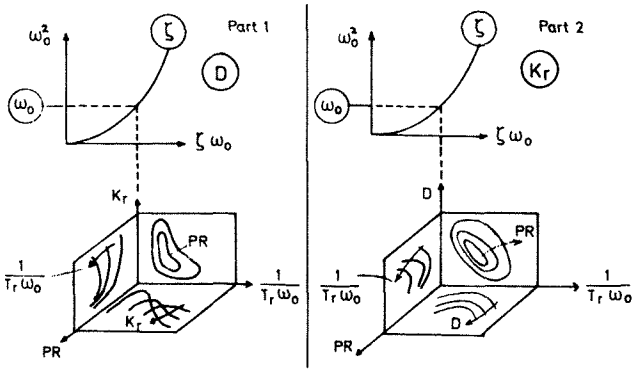

Fig 7. The Simulation Structure (α stipulated)

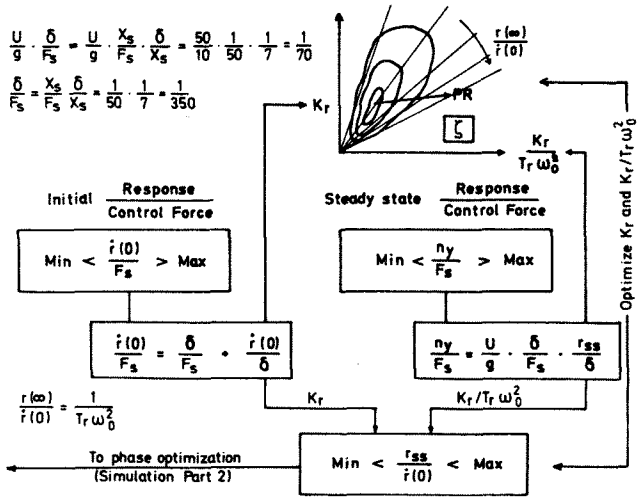

Fig 2. Response Optimization (Simulation Part 1)

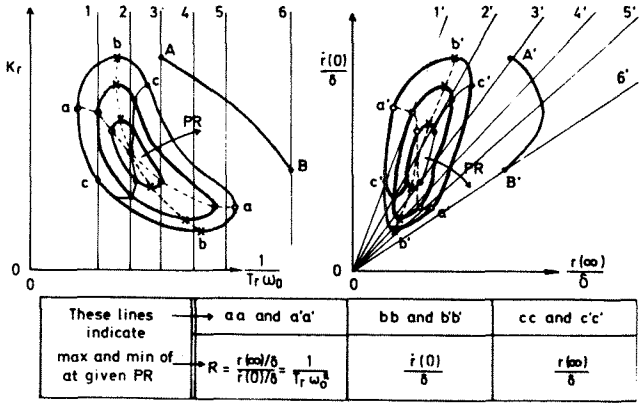

These lines indicate	aa and a'a'	bb and b'b'	cc and c'c'
max and min of at given PR	$R = \frac{r(\infty)/\delta}{\dot r(0)/\delta} = \frac{1}{T_r\omega_0^2}$	$\frac{\dot r(0)}{\delta}$	$\frac{r(\infty)}{\delta}$

Fig 4. Three optima defined by PR = const lines

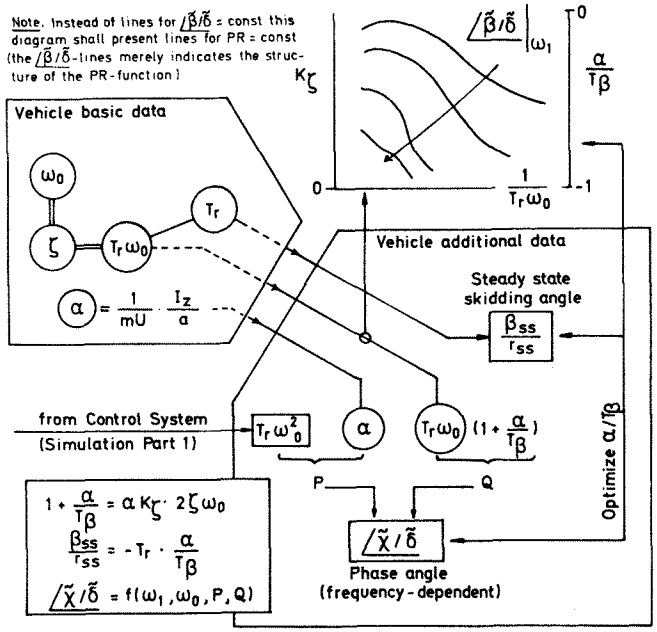

Fig 6. Phase Optimization. (Simulation Part 2)

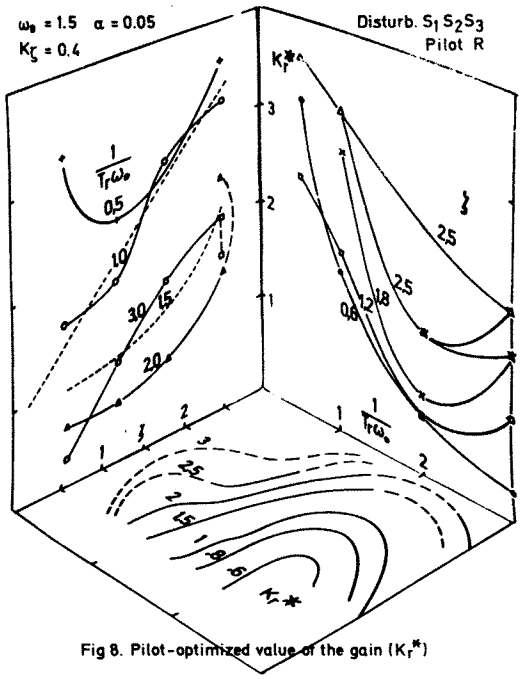

Fig 8. Pilot-optimized value of the gain (K_r^*)

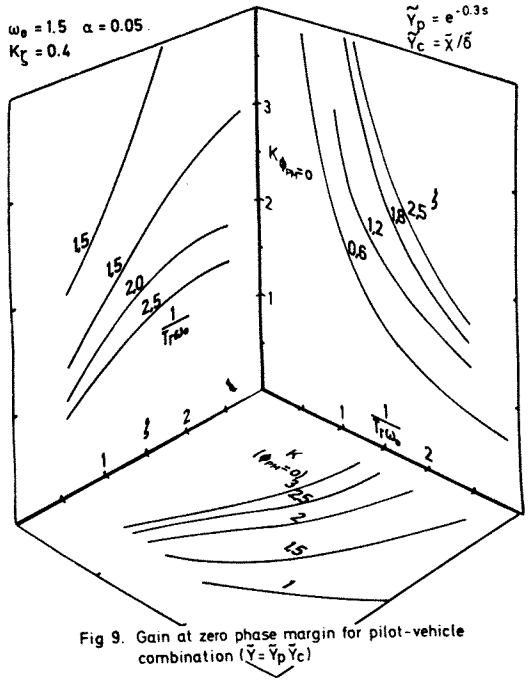

Fig 9. Gain at zero phase margin for pilot-vehicle combination ($\tilde{Y} = \tilde{Y}_p \tilde{Y}_c$)

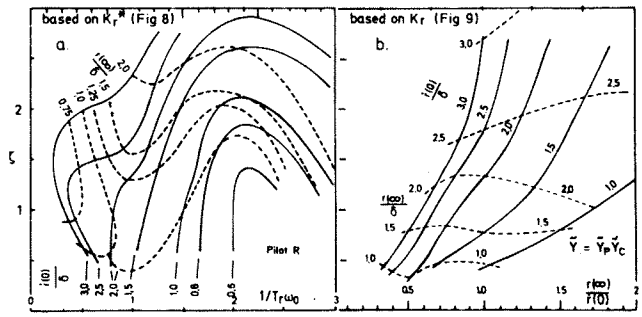

Fig 10. Control response diagram with K_r defined by optimizing condition

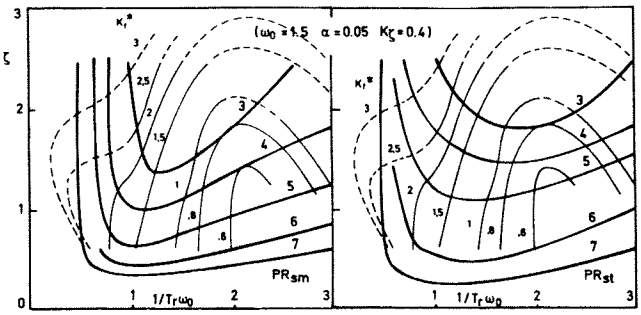

Fig 12. Maneuvering Qualities Plane (Pilot R Disturb. $S_1 S_2 S_3$)

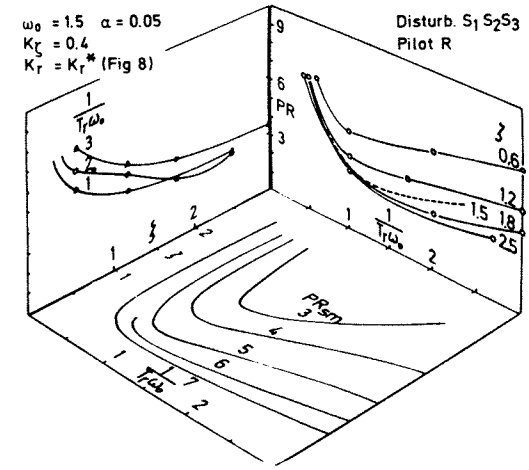

Fig 11. Pilot ratings of ground run maneuvering qualities

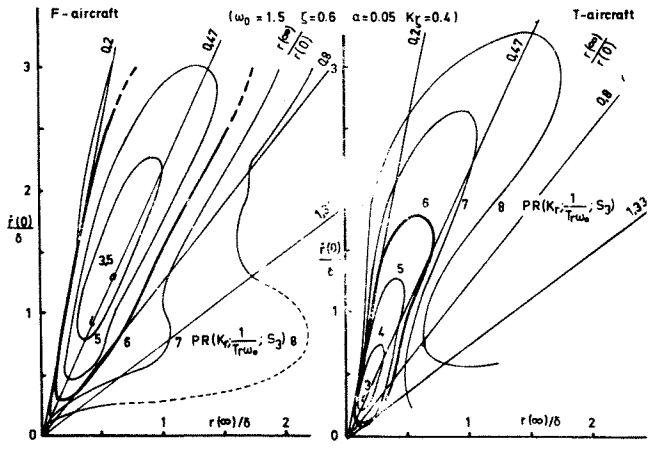

Fig 14. Simulation result of $PR(K_r, 1/T_r\omega_0, S_3)$. Pilot E.

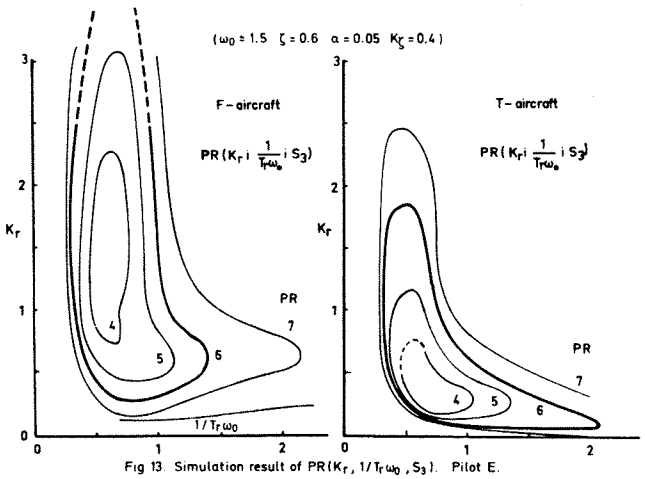

Fig 13. Simulation result of $PR(K_r, 1/T_r\omega_0, S_3)$. Pilot E.

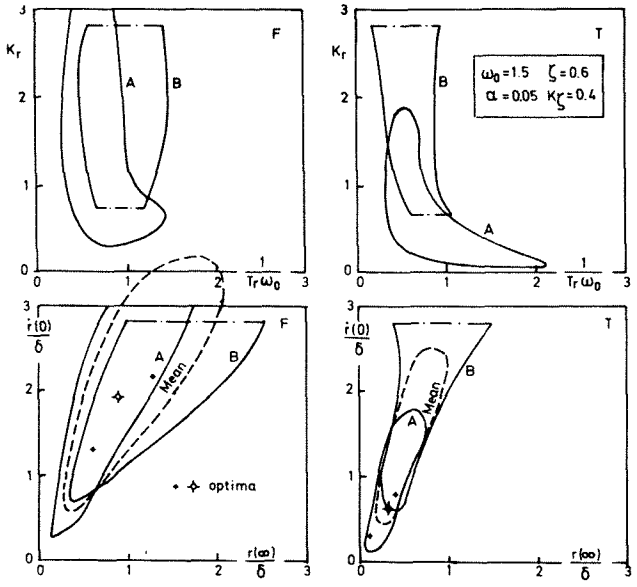

Fig 15. Niveau Charts for PR(S_3) = 6. Pilot E.

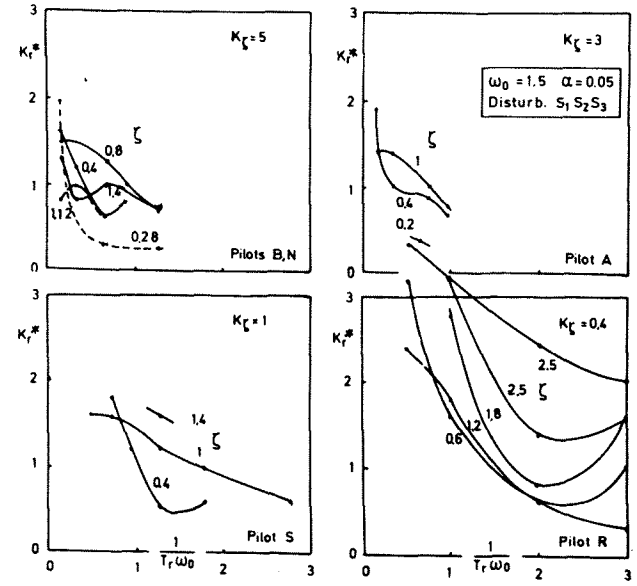

Fig 17. Survey of K_ζ-effects on K_r^*

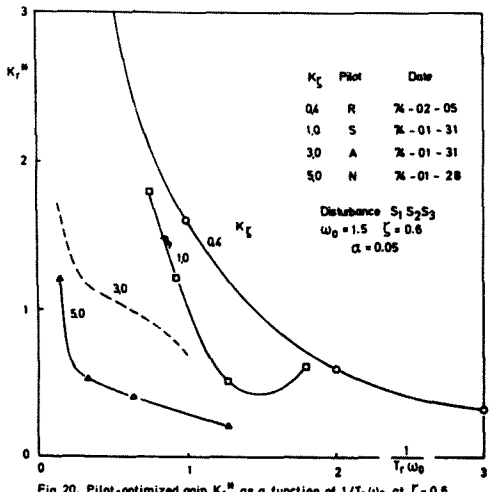

Fig 20. Pilot-optimized gain K_r^* as a function of $1/T_r\omega_0$ at $\zeta = 0.6$ for different K_ζ.

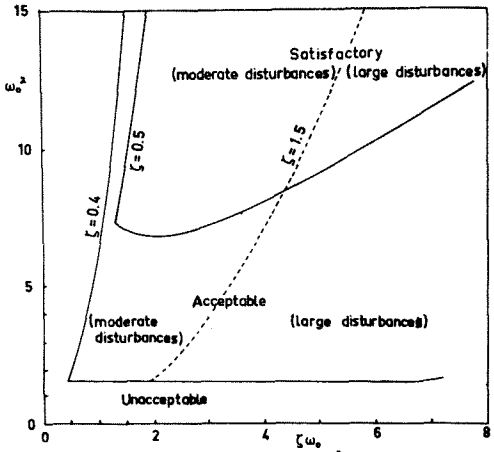

Fig 16. Suggested domains of ω_0^2 and $\zeta\omega_0$

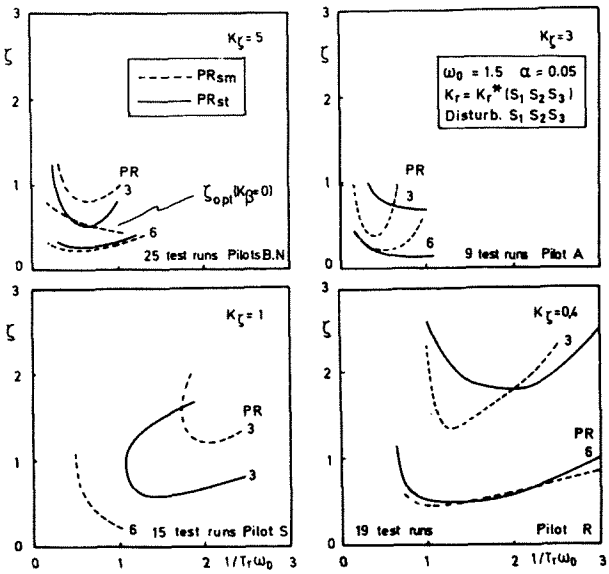

Fig 18. Survey of K_ζ-effects on PR

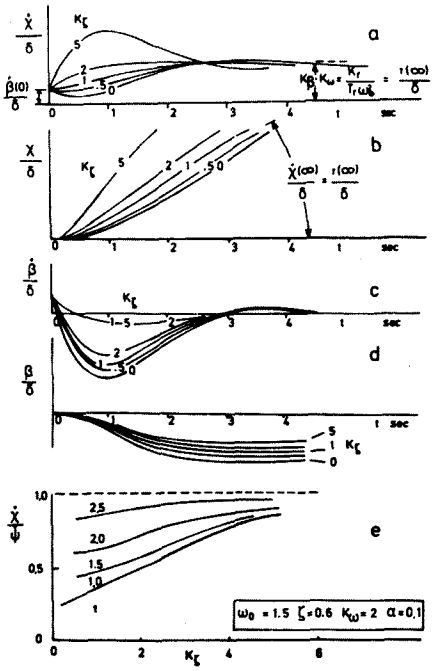

Fig 19. Transient response to step input

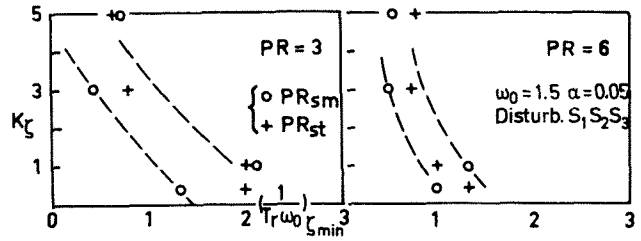

Fig 21. Values of $1/T_r\omega_0$ for optimum PR at ζ = const.

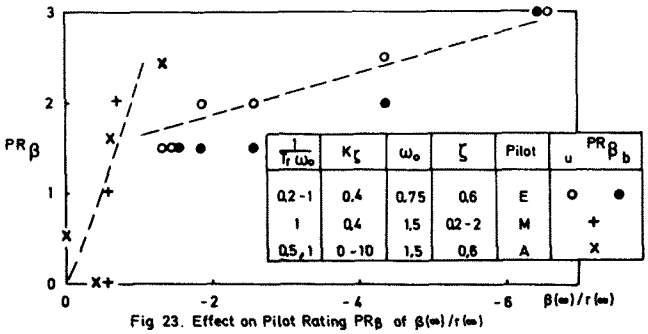

Fig 23. Effect on Pilot Rating PRβ of $\beta(\infty)/r(\infty)$

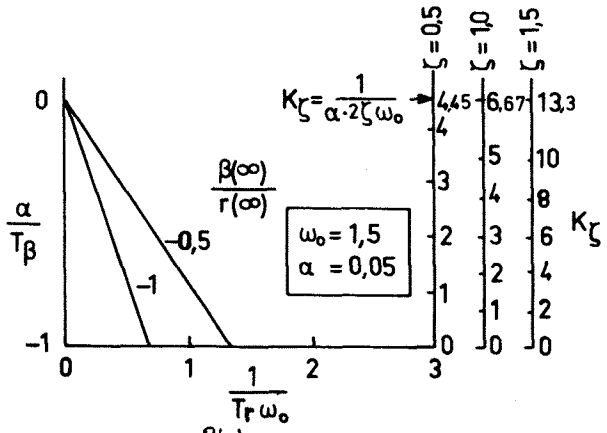

Fig 25. Lines for $\frac{\beta(\infty)}{r(\infty)}$ = const in the $(K_\zeta, \frac{1}{T_r\omega_0})$-system

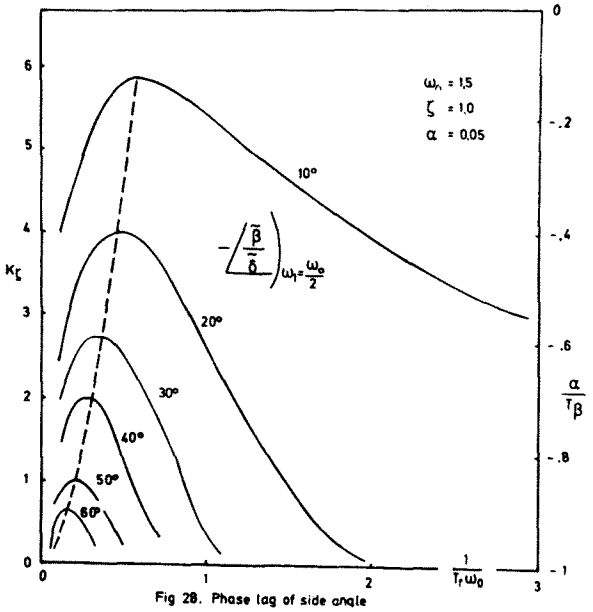

Fig 28. Phase lag of side angle

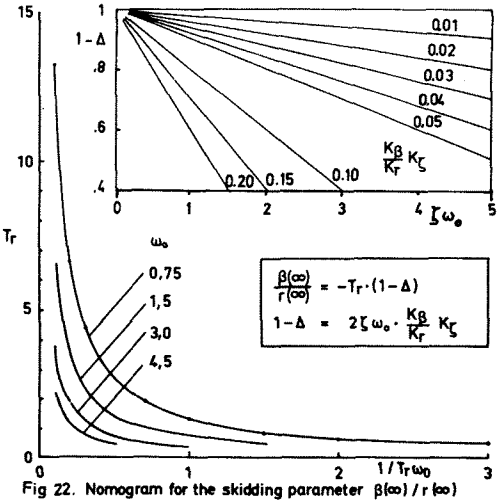

Fig 22. Nomogram for the skidding parameter $\beta(\infty)/r(\infty)$

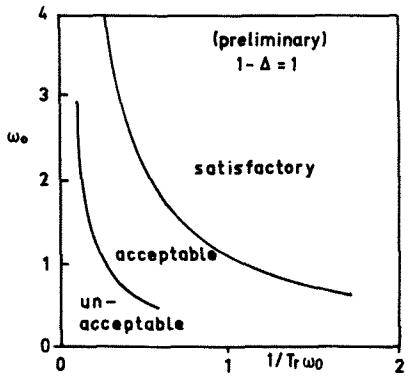

Fig 24. Ranges of $1/T_r\omega_0$ based on skidding

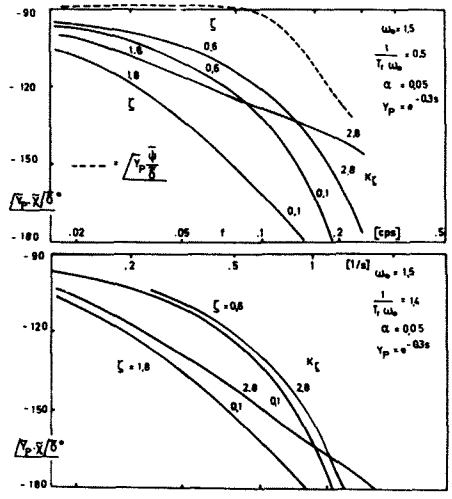

Fig 26. Phase lag of pilot - vehicle combination

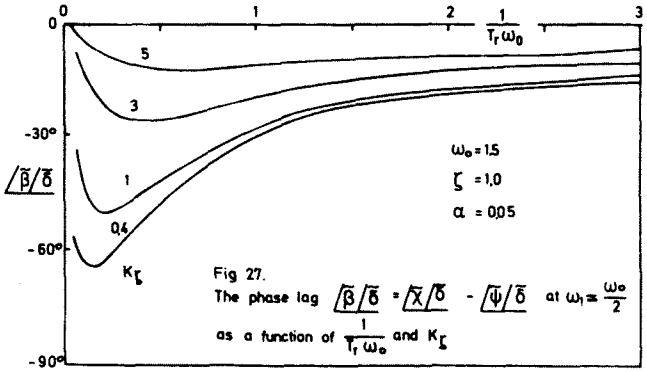

Fig 27.
The phase lag $\overline{\beta/\delta} = \overline{x/\delta} - \overline{\psi/\delta}$ at $\omega_1 = \frac{\omega_o}{2}$
as a function of $\frac{1}{T_r\omega_o}$ and K_ζ

APPENDIX. ON THE SIMULATION PROCEDURE

1. THE SIMULATION TECHNIQUE

1.1 The simulator

The simulator used was the FOSIM research simulator at the Division of Aeronautics, the Royal Institute of Technology, Stockholm (ref 4).

1.2 The pilot task

The pilot controlled the vehicle (aircraft) on a straight runway which was travelled at a constant speed of 50 m/s, the vehicle being subject to disturbances. The control task was to try to keep the vehicle on the runway center line, not with maximum precicion possible, but with pilot-adapted aim concerning precision, and, especially after large diviations, to check these rapidly. Each test run had a duration of 60 seconds. During the run 8 variables were recorded. The following pilot ratings were used i.a.

1. Evaluation of gain parameter K_r during pilot optimization of K_r^* (5 ranks).

2. Pilot rating of maneuvering qualities using the ordinary Cooper-Harper adjective list. The notations PR_{sm} (PR_{st}) were used when the pilot was instructed to use only small (large) control motions.

3. Pilot comments $PR_{\beta u}$, $PR_{\beta b}$ related to the skidding dimension of the vehicles behaviour. (u perception of skidding, b control effort required) (4 ranks).

(An attempt was made to separately assess the control lead-lag-dimension and the overshoot-undershot-dimension by using pilot comments PK_X, PK_Y with adjective list related to the Neal-Smith correlation diagram, ref: AFFDL-TR-70-74. This technique seems promising but requires more calibration testing than could be provided.)

1.3 The pilot inputs

The pilot inputs during the test runs were

- Visual picture of the runway with centerline, bordering lines and cross lines i.e. the variables
  - ψ (distant parts of center- and bordering lines)
  - y_p (near-by parts of center- and bordering lines
  - U (motion pattern of cross lines)

The heading angle (χ) is indirectly available to the pilot by mentally processing the equation

$$\dot{y}_p = U\chi + x_0\dot{\psi}$$

(x_0 = pilot distance ahead of vehicle CG.)

- Pedal force (F_s) and pedal motion (X_s) given by
  - $\partial F_s / \partial X_s = 50$ N/cm
  - $F_{break\ out} = \pm 50$ N when $X_s = 0$
  - max $X_s = \pm 7$ cm, i.e. max $F_s = 350$ N
  - max F_s corresponds to
    - nose wheel angle $\delta = 1$ rad
    - vehicle yaw acceleration, $\dot{r}(0)_{max}$
    - $\dot{r}(0)_{max} = K_r$ = yaw control sensitivity

- Motion by simulator cockpit: Simulation of the centrifugal forces was not possible (mechanical restrictions). In order to make the physical milieu 'alive' to the pilot rolling motions were introduced on y-signals in the computor.

1.4 External disturbances

Three disturbance types, S_1 S_2 S_3, were generated electronically and injected into the system as additions to the vehicle output, thus affecting the visual display input.

Disturbance S_1 was a continous stochastic disturbance in r and β ; White noise, passband filtered between 0.2 and 5 rad/s; $r_{RMS} = 0.013$ rad/s, $\beta_{RMS} = 0.065$ rad. S_1 also was used with 50% reduction of the RMS-values.

Disturbance S_2 was a discrete one-sided one-peaked deviation in r and β with amplitudes 0.05 rad/sec and 0.02 rad injected every 15th second with random sign.

Disturbance S_3 was a discrete step in ψ with amplitude 3 deg injected every 10th second with random sign.

The notation PR(S_1 S_2 S_3) indicates the pilot-averaged value of the pilot rating (PR) from three consecutive runs with S_1 S_2 S_3 acting separately.

1.5 The vehicle parameters

Vehicle parameters relevant for two-dimensional equations of motion are listed in the main report, Table 4.

Comments on data presentation

When the pilot controls the aircraft he perceives combinations of (1) initial, (2) steady state control response, (3) control response ratio, (4) transient control response.

Initial control response is a dominant quality during each (fast) initiation of steering. Its value is the Control Gain K_r. If the maneuver includes a (stationary) curve, also steady state control response is important. Maneuvering along a narrow runway however, hardly produces any full developed steady state turns. Transient control response the pilot continously feels but due to its many inherent parameters it is less suitable for formulating simple design criteria.

For each one of the response characteristica (1) (2) (3) mentioned above three levels can be imagined: too low, acceptable, too high. Thus it is possible to visualize the general lay-out of a definition for acceptable levels for all three characteristica (Fig A-1).

Comments on discrepancies in the simulation environments

In the visual display used true values of yaw angle, side coordinate, heading angle and their derivatives are simulated but it is not possible to check (without large test programs) if the pilot gives these input variables the same relative importance in the simulator as in reality.

In performing simulations for general study irrelevant confusing factors for the pilot should be avoided such as locating the pilot seat far ahead of (or behind) the vehicle center of gravity in which cases the visual heading response is obscured by the yaw rate response.

In the simulations reported the pilot was however located 5.0 m ahead of the vehicles center of gravity. Added to this is the lack of lateral iner-

tia forces as the simulator did not include a motion system with y-motion.

1.6 Simulation pilots

Available for the simulation tests reported were the following pilots

- seven military pilots (O, N, B, A, S, R, M) with experiences from simulation work, during a few hours each
- One civil air line pilot (E), during a few days.

During the first test period a number of pretests were performed by the military pilots while a number of parameters were studied, generally with a different pilot for each test (about 250 test runs).

During the later period series of related pretests were conducted by the civil pilot (about 500 test runs), of which about 110 were related to lane-keeping (not reported in this paper).

2. CONSISTENCY OF THE SIMULATION EVALUATIONS

2.1 Evaluation of K_r and PR

A typical illustration of the inter and intra pilot differences in judging of K_r is shown in Fig A-2. Curves 1 and 2 are for two pilots with nearly the same disturbance function (disturbance S_1 was more annoying to the pilots than S_2 and S_3). Curves 2 and 3 are for one pilot with two intensity levels of the same disturbance type (unsufficient test number to define the 1 σ-dispersion).

The optimum value of PR for the reference configuration ($K_\zeta = 0.4$) is found to be two rank orders better for pilot E(S_3) (Fig 13 F) than for pilot R(S_1 S_2 S_3) (Fig A-2 curve 1 = $\zeta = 0.6$ in Fig 12, 17, 18. It should however be noted that different disturbances were used by the pilots.)

The importance of K_r for the ratings by the same pilot is illustrated in Fig A-3 which shows PR as a function of ζ for four different levels of K_r. The figure shows degenerating PR-values when for the same pilot, the K_r-departure from $K_{r\ nom}$ was increased.

2.2 Pilot task and the FT-distinction

Fig A-4 shows results of pilot rating of maneuvering quality as a function of K_r for pilot E under different conditions.

Pilot E was a commercial air line pilot whose experience of military aircrafts was several years back. This type of mixed background made the pilot produce a considerable dispersion in the ratings during an early phase of the tests (curve a). It then was explicity decided to make two ratings, one under the assumption of a fighter aircraft of the 10-15 tons class, and another assuming a transport aircraft. The pilot then gave separate ratings for F- and T-aircrafts showing reduced dispersion (curves b and c). This procedure is here called the FT-distinction.

2.3 External disturbances

The disturbances $S_1 S_2 S_3$ were considered by the military pilots to be typical for single engined fighter with thrust reverser. S_1 was most annoying and considered unrealistic by the civil pilot. S_3 was least annoying.

Fig A-5 illustrates the pilot rating as a function of K_r for a given configuration. The result shows that the pilot requests larger value of K_r when the disturbances are more annoying. The optimum value of K_r is increased with a factor of about 3 by disturbance S_1 as compared to S_3.

The problem of designing disturbances in specification simulations should be given considerable attention. The experience from this study supports the recommendations from ref 6, i.e. that (at least) two different disturbance spectra should be designed and used in simulation tests.

2.4 The relative damping and the pilot factor

Fig A-6 shows PR-evaluations as functions of ζ made by two pilots, using the same optimum K_r-values, as a function of ζ.

Both pilots agree that low values of ζ are unfavorable but disagree upon the rate of improvement when damping is increased. One pilot finds an optimum at ζ slightly below 1, while the other prefers ζ to be above 2.

2.5 Repeatability

The consistency of pilot rating of maneuvering quality is illustrated in Fig A-7 which shows evaluations by the same pilot made on two consecutive days. Such a comparison is also shown in Fig A-5 above. The dispersion due to this factor is about one rank order.

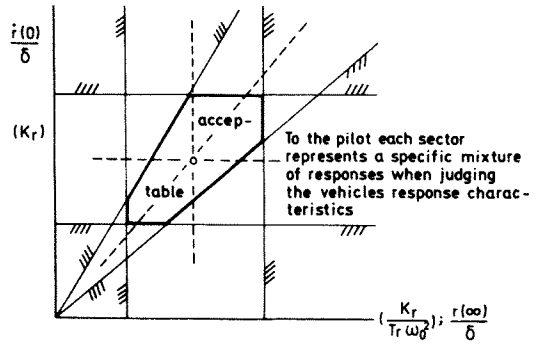

Fig A-1. The pilots rating situation when optimizing K_r or evaluating PR

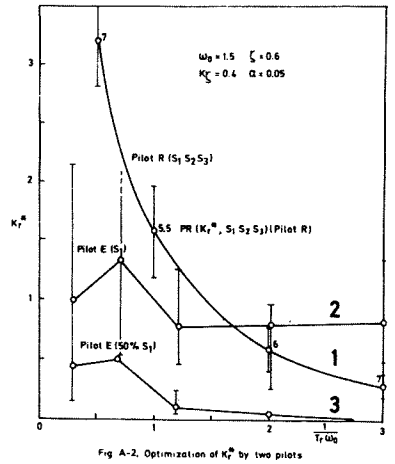

Fig A-2. Optimization of K_r^* by two pilots

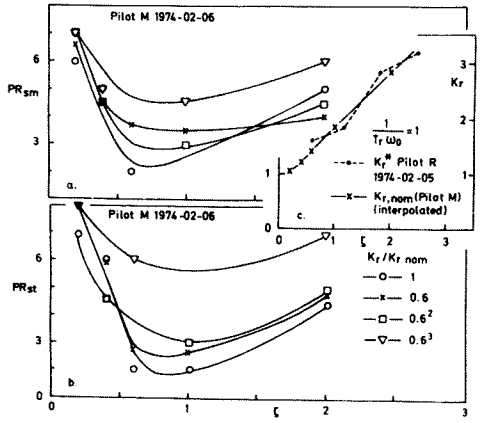

Fig A-3. Pilot rating of maneuvering quality evaluated with K_r equal to different fractions of $K_{r,nom}$

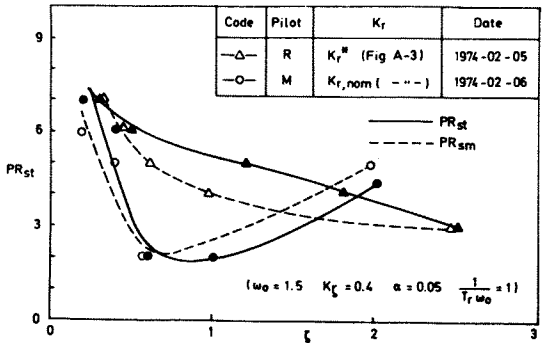

Fig A-6. Evaluation of PR(ζ, $K_{r,opt}$) by two pilots

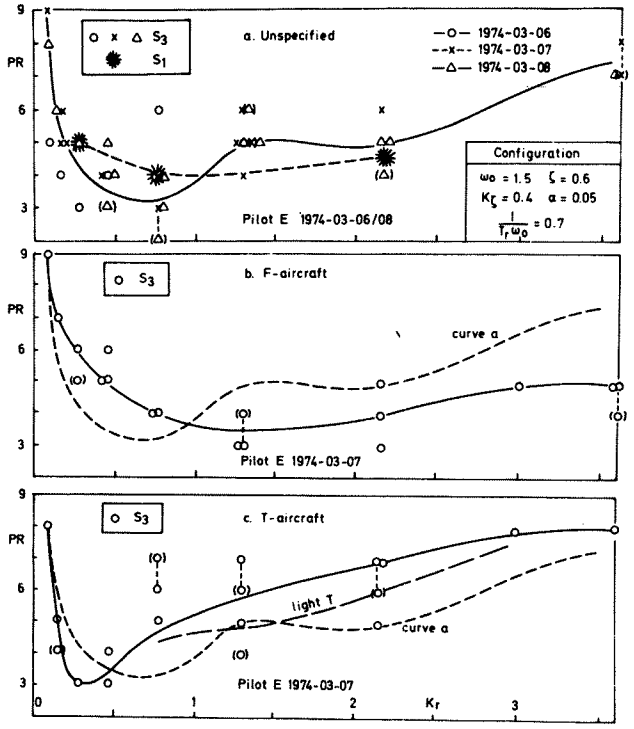

Fig A-4. Evaluation of K for different task types

Disturbance	Code	Test date	Parameters
S_3	○	1974-03-07	$\omega_0 = 1.5$; $\zeta = 0.6$
	△	1974-03-08	$K_\zeta = 1.0$ $\alpha = 0.05$
S_1	■	1974-03-07	$\frac{1}{T_r \omega_0} = 0.7$
	●	1974-03-08	

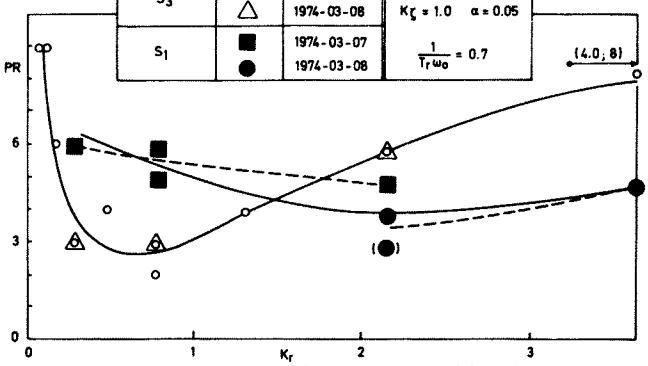

Fig A-5. Optimum K_r is depending on type of disturbance

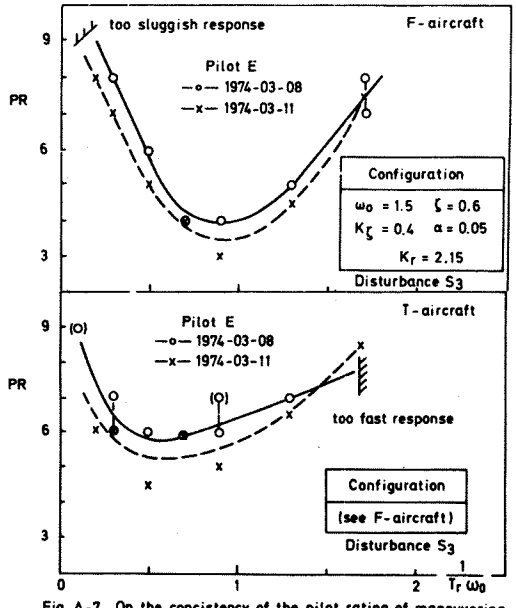

Fig A-7. On the concistency of the pilot rating of maneuvering qualities

SUPPLEMENT. DEGRADING FACTORS FOR THE GROUND RUN MANEUVERING QUALITIES

1. PHYSICAL FACTORS FOR TYRE SIDE FORCES

The physical background for the ground maneuvering capability of the vehicle is the side force (S) on the tyre. The tyre side force is depending on three factors, the tyre vertical load (F_Z), the tyre side-slip angle (ε), and the tyre braking force (B). Typical relationships are shown in Fig S-1. It follows that primary degrading factors for the side force capability are:

- reduction of tyre vertical load; and
- increase of wheel braking force.

Important quality is the local slope of the $S(\varepsilon)$ curve, the side force stiffness. Therefore the following secondary degrading factors should be considered:

- The side force stiffness decreases for increasing side force or slip angle (Fig S-1, points 1.2.3) It follows that side-yaw stability is more critical during stationary turning than during straight path.

- The above mentioned tendency is aggravated by braking. It follows that wheel braking makes the stability and control problems more critical.

- Increasing the braking can cause the side force to vanish discontinously (Fig S-1, points 2' 2'' 2''') It follows that dangerous control situations can occur during wheel braking due to sudden reduction of side friction force.

2. DEGRADING DESIGN FACTORS

2.1 Importance of main wheel side stiffness

An elementary requirement is that ground loop tendencies should be excluded in straight motion. In its simplest form this problem is similar to the weather-cock stability problem. After a yaw angle deviation the side forces on the main wheels (behind the vehicle center of gravity) are stabilizing, the side forces on the nose wheel (in locked position) destabilizing. The primary stability parameter then is the ratio of the side stiffnesses of the nose wheel and the main wheels (C_F/C_R).

Fig S-2 shows that stability can be attained ($SM > 0$) only if the ratio C_F/C_R is below a certain value which is the lower the larger is the parameter a/l that defines the longitudinal distance of the center of gravity behind the nose wheel, expressed as fraction of the vehicle wheel length.

This condition must be satisfied by making C_R large, as C_F can not be reduced below a certain value because of control power requirements in the nose wheel steering. Fig S-3 illustrates the requirements on C_R. The larger the desired values of ω_0 and ζ are (for given values of a/l and SM), the larger is the required value of main wheel side stiffness (C_R).

2.2 Neutral point location and speed effects

In a slightly more rigorous treatment of the stability problem two more factors have to be considered.

The one is that when dynamic stability is considered (as contrasted to the static stability discussed above) a small negative value of the stability margin, called SM_{crit}, is allowed at the stability limit.

The other factor is that aerodynamic forces (which were neglected in the above mentioned discussion) normally have a stabilizing effect that increases in proportion to U^2.

Fig S-4 illustrates the combined effect of these two factors when NP_μ (the neutral point of ground friction forces only) is ahead of the center of gravity.

In its most forward position (NP_A) there are two critical speeds between which the side-yaw motion is divergent.

In a medium position (NP_B) the vehicle becomes marginally stable at a certain speed and has aperiodic convergent eigenmotion at lower speeds and also at higher, up to a certain value above which the eigenmotion becomes periodic and damped.

In a more rearward position (NP_C) the eigenmotion is aperiodic convergent up to a certain speed above which it becomes periodic and damped.

If the NP_μ is located behind the center of gravity the eigenmotion is periodic and damped at all speeds (if aerodynamic forces are stabilizing).

3. DEGRADING OPERATION FACTORS

3.1 Longitudinal load distribution effects

The vertical loads on the nose and the main wheels are affected by

- Inertia effects on pitching moment, due to wheel braking, thrust reverser braking, and to engine thrust; and by
- Aerodynamic effects on total lift and pitching moment due to thrust reverser function (also affecting C_{n_β}), and longitudinal winds or gusts.

Examples of effects and adverse consequences are:

- Increased nose wheel vertical load gives: Reduced side-yaw stability. - Reduced main wheels vertical load gives: Reduced side-yaw stability; reduced wheel braking authority. - Braking of main wheels gives: Increased nose wheel and reduced main wheels vertical load. - Thrust reverser function gives: Changed sum of vertical wheel loads; change of longitudinal wheel load distribution; reduced value of C_{n_β}; asymmetric disturbance forces.

3.2 Lateral load distribution effects

The vertical loads on the left and right main wheels are affected by:

- Inertia effects on rolling moment due to centrifugal forces under different conditions; and by
- Aerodynamic asymmetric forces and moments.

Examples of effects and adverse consequences are:

asymmetric braking forces and side forces, and sudden yawing moment disturbance due to loop effect of tyre side force characteristics.

3.3 Ground friction effects

Factors such as precipitation, temperature, and anomalities causing low or irregular friction effects.

4. DEGRADING FACTORS FROM THE ROLL DEGREE-OF-FREEDOM

If the roll-degree-of-freedom equation is included in the analysis the following effects should be expected (ref 2,3).

The roll eigenmotion is added. This mode is normally well damped. Its frequency should be well above the side-yaw eigenfrequency in order not to interfere with the pilots perception of the side-yaw eigenmotion.

The frequency of the side-yaw eigenmotion is increased (favourable) but its damping is reduced (unfavourable).

If in two degrees-of-freedom a critical speed exists, the inclusion of the roll-degree-of-freedom increases the critical speed (favorable).

The roll-degree-of-freedom introduces a quadratic pole/zero pair in the heading angle transfer function. This is similar to the ω_φ/ω_d-effect evident in the dutch roll mode of an aircraft. The pole and zero may approximately cansel for some configurations but they can in other cases have a significant effect on the closed-loop system characteristics, in cases with relatively light damping. This effect can be stabilizing (favorable) but it can also be destabilizing (unfavorable).

In unbraked motion the roll-degree-of-freedom only has insignificant influence on the steady state control response in yaw rate (favorable).

In braked motion the roll-degree-of-freedom has a strong influence on the steady state yaw rate control response. If the vehicle is understeer in unbraked motion it can be oversteer in braked motion (unfavorable).

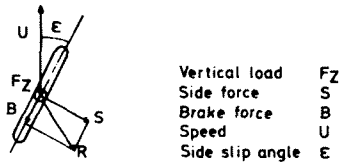

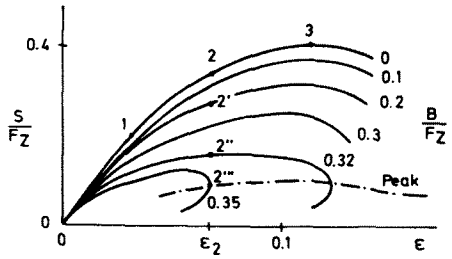

Fig S-1. Ground friction forces on tyres (schematic)

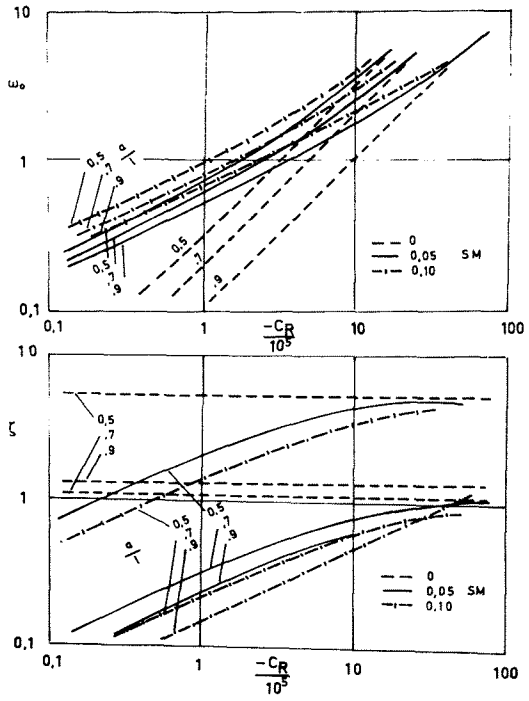

Fig S-3. Nomograms for ω_o and ζ vs $\frac{-C_R}{10^5}$, $\frac{a}{l}$, and SM (typical aircraft) (aerodynamic forces neglected)
$m = 10^5$ kg, $I_z = 10^5$ kg m², $l = 5$ m, $U = 50$ m/s

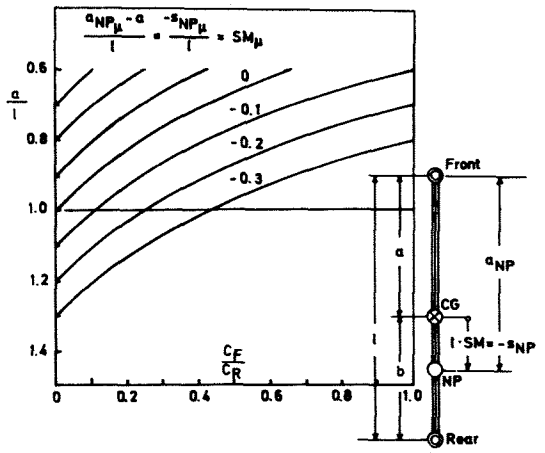

Fig S-2. Relationship between a_{NP_μ}, s_{NP_μ}, SM_μ, and $\frac{C_F}{C_R}$ (only linearized ground friction forces considered)

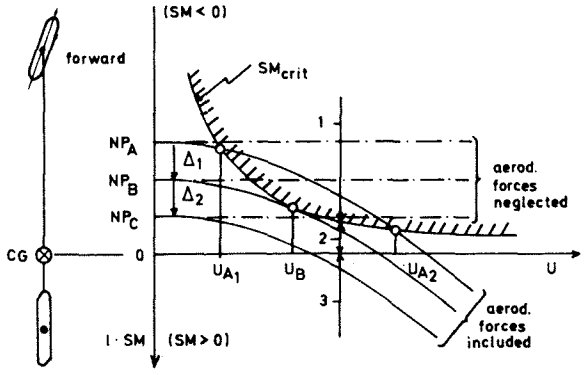

Effect of static margin and aerodynamic forces on critical speed
(Aerodynamic forces are assumed stabilizing in the diagram)

With NP_A the aircraft is stable in yaw for $U < U_{A_1}$ and for $U > U_{A_2}$.

With NP_B the aircraft becomes marginally stable for $U = U_B$.

With NP_C the aircraft becomes stable for all speeds

(With aerodynamic forces neglected or destabilizing all three cases in the figure have critical speeds)

If NP is in region	the yaw-side eigenmotion is
1	aperiodic divergent
2	aperiodic convergent
3	periodic damped

Fig S-4.